

UCSF

UC San Francisco Previously Published Works

Title

ATP-Competitive Inhibitors Midostaurin and Avapritinib Have Distinct Resistance Profiles in Exon 17-Mutant KIT

Permalink

<https://escholarship.org/uc/item/1627w9xi>

Journal

Cancer Research, 79(16)

ISSN

0008-5472

Authors

Apsel Winger, Beth
Cortopassi, Wilian A
Garrido Ruiz, Diego
[et al.](#)

Publication Date

2019-08-15

DOI

10.1158/0008-5472.can-18-3139

Peer reviewed



HHS Public Access

Author manuscript

Cancer Res. Author manuscript; available in PMC 2020 February 15.

Published in final edited form as:

Cancer Res. 2019 August 15; 79(16): 4283–4292. doi:10.1158/0008-5472.CAN-18-3139.

ATP-competitive inhibitors midostaurin and avapritinib have distinct resistance profiles in exon 17-mutant KIT

Beth Apse Winger^a, Wilian A. Cortopassi^b, Diego Garrido Ruiz^b, Lucky Ding^c, Kibeom Jang^c, Ariel Leyte-Vidal^c, Na Zhang^{b,e}, Rosaura Esteve-Puig^{d,*}, Matthew P. Jacobson^b, Neil P. Shah^c

^aDepartment of Pediatrics, Division of Hematology/Oncology, University of California San Francisco, 550 16th Street, Mailstop 0434, San Francisco, CA 94143

^bDepartment of Pharmaceutical Chemistry, University of California San Francisco, Box 2540, 1700 4th St., Byers Hall, Room 408E San Francisco, CA 94143

^cDepartment of Medicine, Division of Hematology/Oncology, University of California San Francisco, 513 Parnassus Avenue, Room S1471, San Francisco CA 94143

^dDepartment of Dermatology, University of California San Francisco, 2340 Sutter Street, N461, Box 0808 San Francisco, California 94143

^eBeijing Key Laboratory of Environmental & Viral Oncology, College of Life Science and Bioengineering, Beijing University of Technology, Beijing, 100124, China

Abstract

KIT is a type-3 receptor tyrosine kinase that is frequently mutated at exon 11 or 17 in a variety of cancers. First generation KIT tyrosine kinase inhibitors (TKIs) are ineffective against KIT exon 17 mutations, which favor an active conformation that prevents these TKIs from binding. The ATP-competitive inhibitors midostaurin and avapritinib, which target the active kinase conformation, were developed to inhibit exon 17-mutant KIT. Because secondary kinase domain mutations are a common mechanism of TKI resistance and guide ensuing TKI design, we sought to define problematic KIT kinase domain mutations for these emerging therapeutics. Midostaurin and avapritinib displayed different vulnerabilities to secondary kinase domain substitutions, with the T670I gatekeeper mutation being selectively problematic for avapritinib. Though gatekeeper mutations often directly disrupt inhibitor binding, we provide evidence that T670I confers avapritinib resistance indirectly by inducing distant conformational changes in the phosphate-binding loop. These findings suggest combining midostaurin and avapritinib may forestall acquired resistance mediated by secondary kinase domain mutations.

Correspondence: neil.shah@ucsf.edu; Ph (415) 476-3303; Fax (415) 476-3726; 513 Parnassus Avenue, Room S1471, San Francisco CA 94143.

*Present Address: Cancer Epigenetics and Biology Program, Bellvitge Biomedical Research Institute, Duran i Reynals Hospital, Barcelona, Spain 08908

Disclosure of Conflicts of Interest

M.P.J. is a consultant to and stockholder of Schrödinger LLC, which licenses, develops, and distributes some of the software used in this work. The other authors declare that no competing interests.

Keywords

KIT; midostaurin; avapritinib; resistance; gatekeeper mutation

Introduction

KIT is a type-3 receptor tyrosine kinase (RTK); other type-3 RTKs are FLT3, PDGFR and CSF1R. Physiologically, KIT is activated by stem cell factor and has multiple downstream effectors, including phosphoinositide-3-kinase (PI3K), RAS/mitogen activated kinase (MAPK), and Janus kinase (JAK)/Signal Transducer and Activator of Transcription (STAT) (1).

KIT is pathologically activated in a variety of cancers. The majority of oncogenic KIT mutations are in exon 11, which encodes the regulatory juxtamembrane (JM) domain, or exon 17, which encodes the activation loop of the kinase domain (2-5). Exon 11 mutations activate KIT by relieving the autoinhibition of the JM domain, while exon 17 mutations shift the conformational equilibrium of the kinase to the active state (6-8). For unclear reasons, exon 11 mutations predominate in gastrointestinal stromal tumor (GIST) and melanoma, whereas exon 17 mutations, exemplified by KIT D816V, predominate in systemic mastocytosis (SM), acute myeloid leukemia (AML) and germinomas (2-5).

Historically, exon 17-mutant KIT has been a challenging drug target while exon 11-mutant KIT has been targetable with clinically available TKIs (1-5,9-11). The first generation of KIT inhibitors (imatinib, sunitinib and regorafenib) transformed GIST driven by exon 11-mutant KIT from a lethal disease to a chronic condition (12). Nonetheless, over 50% of GIST patients relapse with secondary resistance mutations in exon 13 or 14, which encode the drug/ATP binding pocket, or exon 17, which encodes the activation loop (13). In addition, cancers with primary *de novo* exon 17 mutations, such as SM and AML, are insensitive to first generation KIT TKIs because exon 17-mutant KIT is constitutively active and these drugs exclusively bind the inactive conformation (9-11,14,15).

The concept of conformational states affecting TKI binding led to classification of ATP-competitive TKIs as “type 1” or “type 2” (14,16,17). Type 1 TKIs bind the active kinase conformation, whereas type 2 TKIs, which include imatinib, sunitinib and regorafenib, bind the inactive kinase conformation (6,14,15). Inactive conformations are referred to as “DFG-out” conformations because the Mg-binding DFG motif, which commonly makes conformation-specific molecular interactions with TKIs, is oriented out of the active site (6,15-18).

Midostaurin (PKC412) and avapritinib (BLU-285) are the first type 1 TKIs to demonstrate clinical activity in malignancies harboring KIT exon 17 mutations. In April 2017, the US Food and Drug Administration approved midostaurin for advanced systemic mastocytosis (ASM) based on a single-arm, open-label phase 2 trial of midostaurin in heavily pre-treated ASM patients which showed a 60% overall response rate based on modified Valent and Cheson criteria (19). Early phase 1 results of avapritinib in ASM are also encouraging, with a 72% overall response rate in heavily pre-treated patients based on modified IWG-MRT-

ECNM response criteria (20). Though these trials are based on different response criteria, both strongly support the use of KIT-directed therapy in ASM.

Secondary kinase domain mutations are the best-characterized mechanism of acquired resistance to TKIs. These substitutions typically mediate resistance through three mechanisms: (i) directly interfering with TKI binding through steric hindrance or loss of molecular interactions (6,14,18,21), (ii) increasing ATP affinity (22), and/or (iii) destabilizing the kinase conformation required for TKI binding (8,23). One particularly problematic amino acid in kinases, termed the gatekeeper residue, resides in the back of the drug/ATP binding site and controls access to a deep hydrophobic pocket accessed by many TKIs (14,15). Gatekeeper mutations commonly cause TKI resistance and can act through all mechanisms described above (21-27).

Secondary kinase domain mutations capable of conferring resistance to type 1 KIT TKIs have not been previously described (26,28,29). We sought to identify secondary point mutations in KIT D816V that confer resistance to midostaurin and avapritinib with the hope that this knowledge will inform the next iteration of drug development efforts targeting KIT. We assessed candidate mutations for their ability to confer resistance to midostaurin and avapritinib, and determined these drugs have non-overlapping resistance profiles: while T670I, a gatekeeper mutation, confers a high degree of resistance to avapritinib, it retains sensitivity to midostaurin. Computational studies, supported by experimental evidence, unexpectedly predict the KIT T670I gatekeeper mutation can induce distant conformational changes in the P-loop that impair TKI binding, and support the development of next-generation KIT TKIs that minimally interact with the region surrounding the P-loop.

Materials and Methods

Cloning.

KIT was amplified from M230 melanoma cells and cloned into Gateway pENTR1A vector. The D816V mutation was generated by QuikChange (Agilent). MSCVpuro KIT D816V was generated via the LR clonase reaction (30) between pENTR1A-c-KIT D816V and MSCVpuroRFA. Secondary mutations were generated by QuikChange (Agilent), or by digestion and then ligation of purchased gene blocks (Integrated DNA Technologies) containing the desired secondary mutations. All plasmids were verified by diagnostic restriction digest and Sanger sequencing. See supplemental methods for details.

Cell lines.

Parental Ba/F3 cells were purchased from DSMZ. Stable Ba/F3 lines were generated by retroviral spinfection with mutated plasmid as previously described (31). gDNA was extracted from each cell line, KIT was amplified by PCR and sequenced to confirm incorporation of the correct KIT mutant.

Inhibitors.

PKC412/Midostaurin (SelleckChem), avapritinib/BLU-285 (ChemGood), and sunitinib (Sigma) were purchased. Stock solutions were prepared in DMSO and stored at -80°C (avapritinib, sunitinib) or -20°C (midostaurin).

Cell Proliferation.

Cells expressing KIT D816V primary mutations were plated at 2000 cells per well in 96-well white opaque tissue culture plates (Corning) and treated with inhibitor or DMSO. Cells expressing primary V560D mutations were plated at 20,000 cells per well in 25 ng/ml of stem cell factor in 96-well plates and treated with inhibitor or DMSO. After 48 hours, cell proliferation was assessed with the CellTiter-GLO luminescent cell viability assay (Promega). IC50s were calculated with GraphPad Prism 6 software.

Immunoblotting.

Cells were starved for 2 hours, treated with inhibitor or DMSO for 2 hours, then lysed. Lysates were resolved by SDS-PAGE, transferred to nitrocellulose and blotted. See supplemental methods for more details.

Molecular Docking and Molecular Dynamics Simulation.

An active-like conformation of KIT was built based on the ATP-bound structure (PDB ID: 1PKG). Missing domains were added using the SwissModel Server with PDB ID: 3G0E as a reference (8,32,33). Mutations were introduced using the rotamer search implemented in Chimera (34). To generate drug-bound models, ligand was docked into the D816V active site using Gold with midostaurin-DYRK1A complex as a reference (PDB ID: 4NCT) (35). The apo-models were subjected to short-time MD simulations (~11.5 ns) using the AMBER14 suite (36) and the equilibrated structure was used as a reference to maintain an “active-like” form. Models of the apo-double mutants were compared to the models of apo-D816V and drug-bound D816V. ChimeraX (37), a virtual reality tool, was used for 3-dimensional investigation of the structures; PyMol (Shrödinger) was used to generate figures. See supplemental methods for more details.

Results:

Nomination of candidate resistance-conferring mutations for midostaurin and avapritinib.

We previously adapted an XL1-Red *E. coli* saturation mutagenesis assay to identify problematic mutations for TKIs targeting BCR-ABL1 and FLT3, many of which were validated in clinical isolates (31,38-40). However, KIT-containing plasmids are highly unstable in this bacterial strain, rendering this technique unsuitable. Therefore, we generated a targeted panel of *KIT* alleles containing a primary activating exon 17 mutation (D816V) and candidate secondary resistance mutations (Figure 1A). Two complementary methods were used to select candidate resistance mutations. First, we did a literature search for clinically-observed KIT mutations associated with KIT TKI resistance. We identified two categories of mutations (Table S1): activation loop substitutions that favor an active conformation, and alterations in the ATP/drug-binding pocket that sterically and/or

chemically interfere with drug-binding. Given that midostaurin and avapritinib were developed for activation loop mutant KIT, and that the D816V activation loop mutation is the primary mutation for our studies, we reasoned that secondary activation loop mutations were unlikely to confer resistance to these TKIs. In contrast, we hypothesized resistance caused by steric and/or chemical changes within the active site were as likely to impact type 1 TKIs as type 2 TKIs since both are ATP competitive and access the active site. We identified two such secondary mutations discovered in GIST patients who lost response to type 2 TKIs: V654A and T670I (Figure 1A). V654A confers resistance to imatinib and other TKIs by eliminating van der Waals interactions important for drug binding (21). T670I, a gatekeeper mutation (14), confers imatinib resistance by abolishing a hydrogen bond between imatinib and KIT, and through steric hindrance conferred by the extra methyl of the Ile compared to Thr (18,21).

The second method for identifying resistance mutations involved extrapolating from previous work describing resistance mutations in the type-3 RTK FLT3 (40,41). The kinase domains of FLT3 and KIT share 64% sequence identity, and the root-mean-square deviation of the two kinase domains is 0.68 Å, indicating high structural homology (Figure 1A,B). We hypothesized KIT mutations that confer resistance to type 1 KIT TKIs would be analogous to FLT3 mutations that confer resistance to type 1 FLT3 TKIs. We identified three FLT3 mutations that confer resistance to type 1 TKIs: N676K, Y693C, and D698N (Figure 1A). N676K was discovered in a FLT3 internal tandem duplication (ITD)-positive AML patient who relapsed on midostaurin (41). When transduced into 32D cells, FLT3 ITD/N676K confers resistance to midostaurin (41). The analogous mutation in KIT, N655K, has been described in GIST patients, and confers resistance to the type 2 TKI nilotinib (42,43). Two additional resistance mutations, Y693C and D698N, were identified in an *in vitro* saturation mutagenesis screen of FLT3 ITD, and shown to confer resistance to crenolanib and midostaurin, two type 1 FLT3 TKIs (40). The analogous mutations in KIT, Y672C and D677N, have not been reported. Notably, each mutation results from a single nucleotide change, which facilitates the genesis of most clinically-identified resistance mutations. KIT D816V readily transforms Ba/F3 cells to IL-3 independence (Figure S1), and KIT D816V harboring each of these secondary mutations retained transformation potential.

Secondary V654A, N655K and D677N mutations render KIT D816V-driven Ba/F3 cells midostaurin-resistant.

We first determined the sensitivity of our allelic series to midostaurin. Cell proliferation assays confirmed growth of Ba/F3 KIT D816V cells is inhibited by midostaurin in a dose-dependent manner, with an IC₅₀ of 36 nM (Figures 2A, S2A,B). Addition of V654A, T670I, N655K, Y672C or D677N secondary mutations conferred varying degrees of midostaurin resistance relative to D816V alone, with the greatest relative resistance associated with V654A, N655K and D677N (Figure 2A, S2A,B). Consistent with a previous report that demonstrated midostaurin is effective against KIT with a JM domain primary mutation and a T670I secondary mutation (26), KIT D816V/T670I conferred only a 5-fold increase in IC₅₀ compared to D816V alone, similar to the degree of relative resistance conferred by Y672C, but less than any of the other mutants tested. Western blot analysis of phospho-KIT and global phospho-tyrosine confirmed KIT D816V/Y672C and D816V/T670I retain

biochemical sensitivity to midostaurin, but KIT D816V/V654A, D816V/N655K, and D816V/D677N are resistant (Figures 2B-D, S3A-C).

Avapritinib retains activity against midostaurin-resistant mutants but is ineffective against the T670I gatekeeper mutant.

Avapritinib has a strikingly different chemotype than midostaurin (Figure S4). The chemical differences suggest the inhibitors might interact with distinct residues, and display disparate activity against secondary kinase domain mutants. To test this hypothesis, we treated our Ba/F3 KIT mutants with avapritinib. We found the IC₅₀ of avapritinib was 3.8 nM in Ba/F3 KIT D816V cells, which is ten-fold lower than the IC₅₀ of midostaurin (Figures 2E, S2B). Though addition of secondary V654A, N655K, Y672C or D677N mutations resulted in a small increase in IC₅₀ relative to KIT D816V alone, avapritinib generally retained potency against these secondary mutations (IC₅₀s ranging from 1.1 nM to 16 nM) (Figure 2E, S2B). In contrast, the IC₅₀ of avapritinib toward Ba/F3 KIT D816V cells expressing the secondary gatekeeper mutant, T670I, was approximately 70-fold higher (270 nM) than KIT D816V alone (Figure 2E). Western blots examining phosphorylated KIT and global phosphotyrosine confirmed biochemical resistance (Figure 2D).

The impact of secondary V654A and T670I mutations on avapritinib sensitivity is influenced by the nature of the activating primary KIT mutation.

Early clinical trial experience with avapritinib in heavily pre-treated GIST, which commonly harbors primary KIT JM domain mutations (2), shows V654A and T670I mutations are associated with clinical resistance to avapritinib (44). The overall response rate (ORR) in GIST patients with V654A or T670I mutations was 0% (n=25), compared with a 26% ORR (n=84) in patients who lacked these mutations; the stable disease rate was also lower in patients with these mutations (28% vs 51%). Furthermore, the rate of progressive disease was substantially higher in patients with pre-existing V654A or T670I mutations compared with patients who lacked these mutations (72% vs 23%) (44). However, as stated above, our experiments showed avapritinib potently inhibited proliferation of Ba/F3 D816V/V654A cells (IC₅₀ 16 nM; Figures 2E, S2B). We therefore assessed whether the nature of the primary activating mutation in KIT (a JM vs a D816V mutation) influences the potency of avapritinib in KIT mutants with secondary V654A or T670I mutations. We generated KIT alleles with an activating primary V560D mutation, which is a common JM domain substitution in GIST (8), and a secondary V654A or T670I mutation. KIT V560D, and all KIT JM mutants we have tested, are insufficient to transform Ba/F3 cells to IL3 independence (Figure S5). Therefore, experiments were performed in the presence of KIT ligand (stem cell factor; SCF). The IC₅₀ of avapritinib in Ba/F3 KIT V560D cells was over 10-fold greater than the IC₅₀ of avapritinib in Ba/F3 V560D/D816V cells (Figure 3). Notably, the IC₅₀ of avapritinib in Ba/F3 KIT V560D/D816V cells supplemented with SCF was nearly identical to that for Ba/F3 KIT D816V cells without SCF, indicating that the D816V mutation renders KIT highly sensitivity to avapritinib regardless of the presence of SCF (Figure 2E, Figure 3). Ba/F3 KIT V560D cells harboring secondary V654A or T670I substitutions were considerably less sensitive to avapritinib than their counterparts with primary D816V mutations (IC₅₀_{V560D/V654A} 245 nM vs IC₅₀_{D816V/V654A} 16 nM; IC₅₀_{V560D/T670I} 610 nM vs IC₅₀_{D816V/T670I} 270 nM; Figure 3, Figure 2E).

Molecular docking studies predict midostaurin and avapritinib occupy distinct pockets within KIT D816V.

The non-overlapping resistance profiles of midostaurin and avapritinib support the hypothesis that these compounds interact with different residues within the KIT D816V active site, and suggest that avapritinib may interact directly with T670. To investigate potential drug-protein binding interactions, we performed molecular docking studies. We developed a model of apo-KIT D816V using a crystal structure of KIT in the active conformation (PDB: 1PKG) (6), then separately docked midostaurin and avapritinib into the active site (Figure 4A). Both midostaurin and avapritinib are predicted to bind KIT in the interdomain cleft between the N- and C-terminal lobes, consistent with their known ATP-competitive activity. However, because the compounds have distinct shapes, the pockets they are predicted to occupy differ (Figure 4B). Midostaurin, a large bulky compound, projects its 3-pyrroline-2-one head group toward the hinge region, where it is able to make two hydrogen-bonding interactions with the backbone amides of E671 and C673 (Figures 4C, S6A). The phenyl ring of midostaurin's tail extends down from the adenosine-binding pocket and accesses a pocket close to D677. In addition, residues T670 and V654 are positioned to make hydrophobic interactions with midostaurin (Figures 4C, S6A). In contrast, avapritinib occupies a longer, thinner region within the active site (Figures 4B,D), and is predicted to make only one hydrogen bond with the backbone of the hinge region, at residue C673 (Figure 4D, S6B). The docking studies predict an additional hydrogen bond between the primary amine of avapritinib and the side chain carboxylic acid of D810, which is part of the DFG motif (Figure 4D, zoom). The fluorophenyl group of avapritinib is adjacent to the phosphate-binding loop (P-loop), a flexible loop in the active site that helps coordinate the phosphates of ATP during phosphoryl transfer (Figure 4D) (45). The predicted interactions that the DFG and P-loop make with avapritinib are unique compared to midostaurin, which binds far from both these motifs (Figures 4C,D). Despite the observation that the T670I mutation is highly resistant to avapritinib, this TKI is not predicted to bind close to the T670 gatekeeper (Figure 4D).

Molecular dynamics simulations predict mechanisms for resistance-causing mutations.

Molecular docking studies suggest clear differences in how midostaurin and avapritinib bind KIT D816V, providing a rationale for their distinct resistance profiles. However, analysis of residues within 5Å of the docked TKIs, a range that encompasses hydrogen-bonding and hydrophobic interactions, fails to explain how N655K and D677N confer resistance to midostaurin, or how T670I confers resistance to avapritinib (Figures 4C-D, S6).

To elucidate possible structural mechanisms by which these mutations confer resistance, we performed molecular dynamics (MD) simulations. We built models of apo forms of KIT single (D816V) and double (D816V/V654A, D816V/T670I, D816V/N655K, D816V/D677N) mutants, and compared these to the docked poses of midostaurin and avapritinib in D816V. Consistent with previous modeling (21), the V654A mutation is predicted to reduce hydrophobic interactions between residue 654 and the 3-pyrroline-2-one head group of midostaurin (Figures S7A,B). This effect is not observed for avapritinib, which binds more than 5Å from V654 (Figures S6B, S7). The predicted resistance mechanism conferred by mutation of neighboring N655 to lysine appears similar, also reducing hydrophobic

interactions between residue 654 (in this case, the native valine) and midostaurin. In the MD simulation of apo D816V/N655K, the K655 side chain can hydrogen bond to the side chain of neighboring N649, pulling the loop that holds V654 away from the midostaurin-binding pocket, thus reducing the ability of V654 to form hydrophobic interactions with midostaurin and mimicking the effect of the V654A mutation (Figure S7C).

Since gatekeeper residues often interact directly with drugs (e.g. KIT T670 forms an H-bond with imatinib) (6), we initially hypothesized that avapritinib directly interacts with T670, but midostaurin does not. However, our docking studies strongly argue against this hypothesis. In fact, in our model, T670 is more than 5 Å from avapritinib, while the side chain methyl of T670 has favorable close hydrophobic contacts to midostaurin (Figures 4C,D). These hydrophobic interactions between T670 and midostaurin are likely retained upon mutation to the hydrophobic amino acid Ile, and the increased steric bulk of Ile compared to Thr likely explains the small increase in IC₅₀ of midostaurin against the D816V/T670I mutant compared to D816V alone. Since T670I confers a high degree of relative resistance to avapritinib despite being far from avapritinib in our model, and since it appears unlikely that this substitution increases ATP affinity based upon its retention of sensitivity to midostaurin compared to avapritinib, we hypothesized that remote structural changes induced by the gatekeeper mutation might impair avapritinib binding. Structural changes have been ascribed to gatekeeper mutations in kinases, such as ABL and SRC, where gatekeeper mutations push the kinase toward an active conformation through stabilization of a hydrophobic spine (23). By forcing the conformational equilibrium toward the active state, these structural changes contribute to type 2 TKI resistance (23). In KIT, our MD simulations support the hypothesis that T670I alters the conformation of the active site. However, our studies suggest a novel change that involves rigidification of the N-terminal lobe rather than stabilization of a hydrophobic spine. Comparison of the last MD frames of the apo-models of D816V/T670I and D816V predicts the larger aliphatic side chain of I670, compared to native T670, results in increased hydrophobic contacts between residue 670 and residues in proximity of the P-loop (Figures 5A,B). The additional interactions provided by the I670 side chain are predicted to cause a global rigidification of the N-terminal lobe of D816V/T670I compared to D816V, as demonstrated by lower b-factor values for D816V/T670I in the last nanosecond of the simulation compared to D816V alone (Figure S8A,B). The rigidification is predicted to have a profound effect on the conformation of the P-loop, positioning the P-loop closer to the binding pocket of the fluorophenyl moiety of avapritinib (Figure 5C). Changing this pocket should impair avapritinib binding, but not midostaurin binding, because midostaurin does not extend into this pocket, providing a mechanistic hypothesis for why T670I selectively confers resistance to avapritinib.

To test this hypothesis, we generated gatekeeper mutants with varying hydrophobicity. We expected less hydrophobic gatekeeper mutants, such as D816V/T670A, would retain sensitivity to avapritinib, while more hydrophobic gatekeeper mutants, such as D816V/T670V, which has a similar degree of hydrophobicity to Ile, would be resistant. Consistent with these predictions, avapritinib potently inhibited D816V/T670A with an IC₅₀ of 20 nM, but was relatively resistant to the Val gatekeeper substitution (IC₅₀ 360 nM) (Figure 6A). The T670V mutation requires a double amino acid change, which makes it less likely that this mutation will arise clinically. Also consistent with our predictions, D816V/T670A and

D816V/T670V both retain sensitivity to midostaurin, demonstrating increased hydrophobicity of the gatekeeper has no effect on midostaurin as long as the side chain is small enough to avoid steric clash (Figure 6B). Overall, these data support our model that the increased hydrophobicity of Ile causes increased hydrophobic packing that alters the position of the P-loop to selectively impair avapritinib binding.

Discussion

Midostaurin and avapritinib are the first clinically-active type 1 KIT TKIs developed to target exon 17-mutant KIT (19,46). The early clinical efficacy of midostaurin and avapritinib in SM suggests exon 17-mutant KIT represents a driver mutation in this disease. However, identification of secondary resistance mutations to midostaurin and avapritinib in patient isolates is essential to provide definitive proof that exon 17-mutant KIT is a valid drug target, and to guide development of future KIT TKIs. Therefore, we sought to prospectively identify point mutations within the KIT kinase domain that confer resistance to midostaurin and/or avapritinib. We show that in the setting of a primary KIT D816V mutation, midostaurin and avapritinib are susceptible to secondary resistance mutations *in vitro*, but their resistance profiles are distinct. Secondary V654A, N655K and D677N mutations confer resistance to midostaurin, whereas T670I confers selective resistance to avapritinib. Mechanistically, our docking and MD studies predict the V654A mutation acts as previously described (21), conferring resistance by decreasing hydrophobic interactions between V654 and midostaurin. Interestingly, the N655K mutation is also predicted to decrease hydrophobic interactions between residue 654 and midostaurin, via a mechanism that includes formation of a novel hydrogen-bond and concerted conformational changes. The mechanism(s) underlying the selective resistance of D677N to midostaurin is unclear and undergoing further study. Of the mutations assessed, only the T670I gatekeeper mutation confers significant resistance to avapritinib in the setting of a primary KIT D816V mutation. MD simulations suggest a unique resistance mechanism in which the increased hydrophobicity of the Ile compared to Thr leads to rigidification of the N-terminal lobe and movement of the P-loop into the avapritinib binding pocket. In support of this hypothesis, we found substituting T670 for a less hydrophobic amino acid (alanine) results in retention of sensitivity to avapritinib.

Currently, there is limited data on clinical isolates from midostaurin-treated relapsed or refractory patients, and no studies of samples from avapritinib-treated relapsed or refractory patients. A recent clinical study evaluating genetic predictors of midostaurin response demonstrated that midostaurin reduces the KIT D816V allele burden in SM, which represents the strongest on-treatment predictor for improved survival (29). However, mutations in SRSF2, ASXL1 and RUNX1 also have a major impact on midostaurin response, and lack of response was not associated with on-target resistance mutations in KIT (29). This suggests the mutational landscape of SM is complex, an assertion that is further supported by whole exome sequencing (WES) studies that show an average of 35 nonsynonymous mutations per patient with ASM (47). Based on these data, it seems likely that midostaurin's effect may depend, in part, upon oncogenic pathways not involved in canonical KIT signaling. Midostaurin is a derivative of the pan-kinase inhibitor staurosporine, and lacks potency and specificity toward KIT when compared to avapritinib

(46,48). Other targets of midostaurin include FLT3, PDGFRA, PKC and other kinases important in myeloid development (46,49,50). Notably, pharmacokinetic studies show serum concentrations of midostaurin decrease sharply after the first administration in patients, suggesting that midostaurin induces its own metabolism and may not maintain high enough concentrations in the blood to sustain KIT inhibition beyond the initial treatment period (51). Given data from over a decade of experience with midostaurin, it is likely that its moderate efficacy and lack of on-target resistance mutations in SM result from the combination of poor pharmacokinetic properties, low potency and general lack of specificity for KIT in a disease with significant genetic complexity (29,52).

In contrast, avapritinib is a highly selective and potent KIT inhibitor (46). Though the genetic complexity of SM may pose a challenge for the success of all KIT-targeted therapies in SM, the early success of avapritinib in SM strongly suggests that avapritinib is exerting its effect through KIT inhibition, and that avapritinib may apply sufficient pressure on the disease to select for resistance-conferring KIT mutants. In addition, comparison of WES in GIST with WES in SM shows GIST has a higher mutational burden than SM (35-60 mutations/sample in GIST vs 25 mutations/sample in SM) (47,53,54). Given that GIST is at least as genetically complex as SM, and that resistance to KIT TKIs in GIST often involves on-target KIT mutations, it seems plausible that on-target mutations will confer avapritinib resistance in SM. In addition, AML has been shown to harbor relatively few mutations in coding regions (55), and the potency of avapritinib may enable the first assessment of exon 17-mutant KIT as an oncogenic driver mutation in this disease. An analogous scenario was observed in the validation of FLT3 as a drug target in FLT3-ITD-positive AML. In that disease, the first several FLT3 inhibitors, including midostaurin, failed to achieve deep responses, raising the possibility that pathologically activated FLT3 was not a disease driver. Subsequently, quizartinib, the first potent and selective inhibitor of FLT3-ITD, was shown to induce deep remissions in a substantial proportion of patients (56). Moreover, acquired resistance to quizartinib was highly associated with secondary resistance mutations in FLT3-ITD, thus validating FLT3-ITD as a therapeutic target and driver of AML (31,57).

The ability of secondary mutations to confer clinical resistance to targeted therapeutics is highly dependent upon the concentration of drug safely achievable in patients. Only translational studies of clinical isolates obtained from patients with acquired resistance to targeted therapy can provide definitive evidence for the clinical importance of candidate resistance mutations. We found the high nanomolar concentration of avapritinib required to inhibit the proliferation of Ba/F3 KIT D816V/T670I cells is similar to the concentration of avapritinib required to inhibit the proliferation of Ba/F3 KIT V560D/V654A cells. Since the V654A mutation in GIST patients with JM mutant KIT is associated with clinical resistance to avapritinib (44), our studies point to the T670I mutation in KIT D816V as a candidate mediator of acquired clinical resistance to avapritinib. Avapritinib is the most potent and selective type 1 KIT TKI described to date, and our data suggest that the KIT D816V/T670I mutant is a high-value target for efforts to rationally design the next generation of potent type 1 KIT TKIs. Our MD simulations predict the T670I mutation induces resistance to avapritinib through a novel mechanism involving neither steric clash nor increased ATP affinity, two previously implicated resistance mechanisms for gatekeeper mutations. Rather, MD simulations predict distant conformational changes in the P-loop that contract the drug-

accessible area adjacent to this region are primarily responsible for avapritinib resistance. These data support the development of potent type 1 KIT inhibitors that not only avoid interactions with T670, but can tolerate significant flexibility in the P-loop, or perhaps avoid interaction with this region altogether. Moreover, it is possible that gatekeeper mutations may impact the P-loop region in other kinases, and as efforts are undertaken to develop TKIs that retain activity against gatekeeper mutants in a broad range of kinases, it may be important to consider the potential impacts of gatekeeper substitutions on P-loop architecture. In addition, we provide rationale for clinically assessing midostaurin and avapritinib as second-line therapeutics for select secondary KIT mutations that arise upon initial treatment with the other agent. In light of the non-overlapping resistance profiles of avapritinib and midostaurin, and the challenges of finding a single drug that can overcome the complexity of KIT TKI-resistance, strategies that combine avapritinib with either midostaurin or a more potent type 1 TKI that retains activity against T670I, may forestall the development of clinical resistance and warrant clinical investigation in patients with malignancies harboring exon 17-mutant KIT.

Supplementary Material

Refer to Web version on PubMed Central for supplementary material.

Acknowledgments

Grant Support: National Cancer Institute CA176091 (to NPS); St. Baldrick's Foundation Award ID: 527421 and the Frank A. Campini Foundation (BAW); The China Scholarship Council Award Grant No. 201706545010 (NZ); this work used the Extreme Science and Engineering Discovery Environment (XSEDE), which is supported by National Science Foundation Grant No. ACI-1548562 (MPJ); NPS acknowledges the generous support of the Yen family. We gratefully thank Kevin Shannon, Kevan Shokat, Jonathan Winger and Debajyoti Datta for helpful discussions.

References

1. Lennartsson J, Ronnstrand L. Stem cell factor receptor/c-Kit: from basic science to clinical implications. *Physiol Rev* 2012;92:1619–49. [PubMed: 23073628]
2. Hirota S, Isozaki K, Moriyama Y, Hashimoto K, Nishida T, Ishiguro S, et al. Gain-of-function mutations of c-kit in human gastrointestinal stromal tumors. *Science* 1998;279:577–80. [PubMed: 9438854]
3. Nagata H, Worobec AS, Oh CK, Chowdhury BA, Tannenbaum S, Suzuki Y, et al. Identification of a point mutation in the catalytic domain of the protooncogene c-kit in peripheral blood mononuclear cells of patients who have mastocytosis with an associated hematologic disorder. *Proc Natl Acad Sci U S A* 1995;92:10560–4. [PubMed: 7479840]
4. Willmore-Payne C, Holden JA, Tripp S, Layfield LJ. Human malignant melanoma: detection of BRAF- and c-kit-activating mutations by high-resolution amplicon melting analysis. *Hum Pathol* 2005;36:486–93. [PubMed: 15948115]
5. Wang L, Yamaguchi S, Burstein MD, Terashima K, Chang K, Ng HK, et al. Novel somatic and germline mutations in intracranial germ cell tumours. *Nature* 2014;511:241–5. [PubMed: 24896186]
6. Mol CD, Dougan DR, Schneider TR, Skene RJ, Kraus ML, Scheibe DN, et al. Structural basis for the autoinhibition and STI-571 inhibition of c-Kit tyrosine kinase. *J Biol Chem* 2004;279:31655–63. [PubMed: 15123710]
7. Chan PM, Ilangumaran S, La Rose J, Chakrabarty A, Rottapel R. Autoinhibition of the kit receptor tyrosine kinase by the cytosolic juxtamembrane region. *Mol Cell Biol* 2003;23:3067–78. [PubMed: 12697809]

8. Gajiwala KS, Wu JC, Christensen J, Deshmukh GD, Diehl W, DiNitto JP, et al. KIT kinase mutants show unique mechanisms of drug resistance to imatinib and sunitinib in gastrointestinal stromal tumor patients. *Proc Natl Acad Sci U S A* 2009;106:1542–7. [PubMed: 19164557]
9. Cortes J, Giles F, O'Brien S, Thomas D, Albitar M, Rios MB, et al. Results of imatinib mesylate therapy in patients with refractory or recurrent acute myeloid leukemia, high-risk myelodysplastic syndrome, and myeloproliferative disorders. *Cancer* 2003;97:2760–6. [PubMed: 12767088]
10. Pardanani A, Elliott M, Reeder T, Li CY, Baxter EJ, Cross NC, et al. Imatinib for systemic mast-cell disease. *Lancet* 2003;362:535–6. [PubMed: 12932387]
11. Vega-Ruiz A, Cortes JE, Sever M, Manshoury T, Quintas-Cardama A, Luthra R, et al. Phase II study of imatinib mesylate as therapy for patients with systemic mastocytosis. *Leuk Res* 2009;33:1481–4. [PubMed: 19193436]
12. Demetri GD, von Mehren M, Blanke CD, Van den Abbeele AD, Eisenberg B, Roberts PJ, et al. Efficacy and safety of imatinib mesylate in advanced gastrointestinal stromal tumors. *N Engl J Med* 2002;347:472–80. [PubMed: 12181401]
13. Antonescu CR, Besmer P, Guo T, Arkun K, Hom G, Koryotowski B, et al. Acquired resistance to imatinib in gastrointestinal stromal tumor occurs through secondary gene mutation. *Clin Cancer Res* 2005;11:4182–90. [PubMed: 15930355]
14. Dar AC, Shokat KM. The evolution of protein kinase inhibitors from antagonists to agonists of cellular signaling. *Annu Rev Biochem* 2011;80:769–95. [PubMed: 21548788]
15. Krishnamurty R, Maly DJ. Biochemical mechanisms of resistance to small-molecule protein kinase inhibitors. *ACS Chem Biol* 2010;5:121–38. [PubMed: 20044834]
16. Nagar B, Bornmann WG, Pellicena P, Schindler T, Veach DR, Miller WT, et al. Crystal structures of the kinase domain of c-Abl in complex with the small molecule inhibitors PD173955 and imatinib (STI-571). *Cancer Res* 2002;62:4236–43. [PubMed: 12154025]
17. Okram B, Nagle A, Adrian FJ, Lee C, Ren P, Wang X, et al. A general strategy for creating “inactive-conformation” abl inhibitors. *Chem Biol* 2006;13:779–86 [PubMed: 16873026]
18. Schindler T, Bornmann W, Pellicena P, Miller WT, Clarkson B, Kuriyan J. Structural mechanism for STI-571 inhibition of abelson tyrosine kinase. *Science* 2000;289:1938–42. [PubMed: 10988075]
19. Gotlib J, Kluin-Nelemans HC, George TI, Akin C, Sotlar K, Hermine O, et al. Efficacy and Safety of Midostaurin in Advanced Systemic Mastocytosis. *N Engl J Med* 2016;374:2530–41. [PubMed: 27355533]
20. DeAngelo DJ, Quiery AT, Radia D, Drummond MW, Gotlib J, Robinson WA, et al. Clinical activity in a Phase 1 study of BLU-285, a potent, highly-selective inhibitor of KIT D816V in advanced systemic mastocytosis. American Society of Hematology Annual Meeting, Atlanta, GA USA 2017.
21. Garner AP, Gozgit JM, Anjum R, Vodala S, Schrock A, Zhou T, et al. Ponatinib inhibits polyclonal drug-resistant KIT oncoproteins and shows therapeutic potential in heavily pretreated gastrointestinal stromal tumor (GIST) patients. *Clin Cancer Res* 2014;20:5745–55. [PubMed: 25239608]
22. Yun CH, Mengwasser KE, Toms AV, Woo MS, Greulich H, Wong KK, et al. The T790M mutation in EGFR kinase causes drug resistance by increasing the affinity for ATP. *Proc Natl Acad Sci U S A* 2008;105:2070–5. [PubMed: 18227510]
23. Azam M, Seeliger MA, Gray NS, Kuriyan J, Daley GQ. Activation of tyrosine kinases by mutation of the gatekeeper threonine. *Nat Struct Mol Biol* 2008;15:1109–18. [PubMed: 18794843]
24. Branford S, Rudzki Z, Walsh S, Grigg A, Arthur C, Taylor K, et al. High frequency of point mutations clustered within the adenosine triphosphate-binding region of BCR/ABL in patients with chronic myeloid leukemia or Ph-positive acute lymphoblastic leukemia who develop imatinib (STI571) resistance. *Blood* 2002;99:3472–5. [PubMed: 11964322]
25. Choi YL, Soda M, Yamashita Y, Ueno T, Takashima J, Nakajima T, et al. EML4-ALK mutations in lung cancer that confer resistance to ALK inhibitors. *N Engl J Med* 2010;363:1734–9. [PubMed: 20979473]
26. Debiec-Rychter M, Cools J, Dumez H, Sciot R, Stul M, Mentens N, et al. Mechanisms of resistance to imatinib mesylate in gastrointestinal stromal tumors and activity of the PKC412

- inhibitor against imatinib-resistant mutants. *Gastroenterology* 2005;128:270–9. [PubMed: 15685537]
27. Pao W, Miller VA, Politi KA, Riely GJ, Somwar R, Zakowski MF, et al. Acquired resistance of lung adenocarcinomas to gefitinib or erlotinib is associated with a second mutation in the EGFR kinase domain. *PLoS Med* 2005;2:e73. [PubMed: 15737014]
 28. Gotlib J A molecular roadmap for midostaurin in mastocytosis. *Blood* 2017;130:98–100. [PubMed: 28705853]
 29. Jawhar M, Schwaab J, Naumann N, Horny HP, Sotlar K, Haferlach T, et al. Response and progression on midostaurin in advanced systemic mastocytosis: KIT D816V and other molecular markers. *Blood* 2017;130:137–45. [PubMed: 28424161]
 30. Katzen F Gateway((R)) recombinational cloning: a biological operating system. *Expert Opin Drug Discov* 2007;2:571–89. [PubMed: 23484762]
 31. Smith CC, Wang Q, Chin CS, Salerno S, Damon LE, Levis MJ, et al. Validation of ITD mutations in FLT3 as a therapeutic target in human acute myeloid leukaemia. *Nature* 2012;485:260–3. [PubMed: 22504184]
 32. Guex N, Peitsch MC, Schwede T. Automated comparative protein structure modeling with SWISS-MODEL and Swiss-PdbViewer: a historical perspective. *Electrophoresis* 2009;30 Suppl 1:S162–73. [PubMed: 19517507]
 33. Mol CD, Lim KB, Sridhar V, Zou H, Chien EY, Sang BC, et al. Structure of a c-kit product complex reveals the basis for kinase transactivation. *J Biol Chem* 2003;278:31461–4. [PubMed: 12824176]
 34. Pettersen EF, Goddard TD, Huang CC, Couch GS, Greenblatt DM, Meng EC, et al. UCSF Chimera--a visualization system for exploratory research and analysis. *J Comput Chem* 2004;25:1605–12. [PubMed: 15264254]
 35. Alexeeva M, Aberg E, Engh RA, Rothweiler U. The structure of a dual-specificity tyrosine phosphorylation-regulated kinase 1A-PKC412 complex reveals disulfide-bridge formation with the anomalous catalytic loop HRD(HCD) cysteine. *Acta Crystallogr D Biol Crystallogr* 2015;71:1207–15. [PubMed: 25945585]
 36. Case DA, Babin V, Berryman JT, Betz RM, Cai Q, Cerutti DS, et al. {Amber 14}. 2014.
 37. Goddard TD, Huang CC, Meng EC, Pettersen EF, Couch GS, Morris JH, et al. UCSF ChimeraX: Meeting modern challenges in visualization and analysis. *Protein Science* 2018;27:14–25. [PubMed: 28710774]
 38. Azam M, Latek RR, Daley GQ. Mechanisms of autoinhibition and STI-571/imatinib resistance revealed by mutagenesis of BCR-ABL. *Cell* 2003;112:831–43. [PubMed: 12654249]
 39. Burgess MR, Skaggs BJ, Shah NP, Lee FY, Sawyers CL. Comparative analysis of two clinically active BCR-ABL kinase inhibitors reveals the role of conformation-specific binding in resistance. *Proc Natl Acad Sci U S A* 2005;102:3395–400. [PubMed: 15705718]
 40. Smith CC, Lasater EA, Lin KC, Wang Q, McCreery MQ, Stewart WK, et al. Crenolanib is a selective type I pan-FLT3 inhibitor. *Proc Natl Acad Sci U S A* 2014;111:5319–24. [PubMed: 24623852]
 41. Heidel F, Solem FK, Breitenbuecher F, Lipka DB, Kasper S, Thiede MH, et al. Clinical resistance to the kinase inhibitor PKC412 in acute myeloid leukemia by mutation of Asn-676 in the FLT3 tyrosine kinase domain. *Blood* 2006;107:293–300. [PubMed: 16150941]
 42. Kinoshita K, Hirota S, Isozaki K, Nishitani A, Tsutsui S, Watabe K, et al. Characterization of tyrosine kinase I domain c-kit gene mutation Asn655Lys newly found in primary jejunal gastrointestinal stromal tumor. *Am J Gastroenterol* 2007;102:1134–6.
 43. Sugase T, Takahashi T, Ishikawa T, Ichikawa H, Kanda T, Hirota S, et al. Surgical resection of recurrent gastrointestinal stromal tumor after interruption of long-term nilotinib therapy. *Surg Case Rep* 2016;2:137. [PubMed: 27864817]
 44. Heinrich M, von Mehren M, Jones RL, Bauer S, Kang Y, Schöffski P, et al. Avapritinib is Highly Active and Well-tolerated in Patients With Advanced GIST Driven by Diverse Variety of Oncogenic Mutations in KIT and PDGFRA. 2018 11 15, 2018; Rome, Italy.
 45. Huse M, Kuriyan J. The conformational plasticity of protein kinases. *Cell* 2002;109:275–82. [PubMed: 12015977]

46. Evans EK, Gardino AK, Kim JL, Hodous BL, Shutes A, Davis A, et al. A precision therapy against cancers driven by KIT/PDGFRA mutations. *Sci Transl Med* 2017;9.
47. Soverini S, De Benedittis C, Rondoni M, Papayannidis C, Ficarra E, Paciello G, et al. The Genomic and Transcriptomic Landscape of Systemic Mastocytosis. *Blood* 2016;128.
48. Manley PW, Weisberg E, Sattler M, Griffin JD. Midostaurin, a Natural Product-Derived Kinase Inhibitor Recently Approved for the Treatment of Hematological Malignancies. Published as part of the Biochemistry series "Biochemistry to Bedside". *Biochemistry* 2018;57:477–8. [PubMed: 29188995]
49. Fabbro D, Ruetz S, Bodis S, Pruschy M, Csermak K, Man A, et al. PKC412--a protein kinase inhibitor with a broad therapeutic potential. *Anticancer Drug Des* 2000;15:17–28. [PubMed: 10888033]
50. Fabbro D, Buchdunger E, Wood J, Mestan J, Hofmann F, Ferrari S, et al. Inhibitors of protein kinases: CGP 41251, a protein kinase inhibitor with potential as an anticancer agent. *Pharmacol Ther* 1999;82:293–301. [PubMed: 10454207]
51. Propper DJ, McDonald AC, Man A, Thavasu P, Balkwill F, Braybrooke JP, et al. Phase I and pharmacokinetic study of PKC412, an inhibitor of protein kinase C. *J Clin Oncol* 2001;19:1485–92. [PubMed: 11230495]
52. Gotlib J, Berube C, Growney JD, Chen CC, George TI, Williams C, et al. Activity of the tyrosine kinase inhibitor PKC412 in a patient with mast cell leukemia with the D816V KIT mutation. *Blood* 2005;106:2865–70. [PubMed: 15972446]
53. Ami EB, Kamran SC, George S, Morgan JA, Wagner AJ, Merriam P, et al. Whole exome analysis of patients (pts) with metastatic GIST (mGIST) demonstrating exceptional survival with imatinib (IM) therapy compared to those with short term benefit. *Journal of Clinical Oncology* 2017.
54. Kang G, Yun H, Sun CH, Park I, Lee S, Kwon J, et al. Integrated genomic analyses identify frequent gene fusion events and VHL inactivation in gastrointestinal stromal tumors. *Oncotarget* 2016;7:6538–51. [PubMed: 25987131]
55. Alexandrov LB, Nik-Zainal S, Wedge DC, Aparicio SA, Behjati S, Biankin AV, et al. Signatures of mutational processes in human cancer. *Nature* 2013;500:415–21. [PubMed: 23945592]
56. Cortes JE, Kantarjian H, Foran JM, Ghirdaladze D, Zodelava M, Borthakur G, et al. Phase I study of quizartinib administered daily to patients with relapsed or refractory acute myeloid leukemia irrespective of FMS-like tyrosine kinase 3-internal tandem duplication status. *J Clin Oncol* 2013;31:3681–7. [PubMed: 24002496]
57. Alvarado Y, Kantarjian HM, Luthra R, Ravandi F, Borthakur G, Garcia-Manero G, et al. Treatment with FLT3 inhibitor in patients with FLT3-mutated acute myeloid leukemia is associated with development of secondary FLT3-tyrosine kinase domain mutations. *Cancer* 2014;120:2142–9. [PubMed: 24737502]
58. Kyte J, Doolittle RF. A simple method for displaying the hydropathic character of a protein. *J Mol Biol* 1982;157:105–32. [PubMed: 7108955]

Statement of Significance

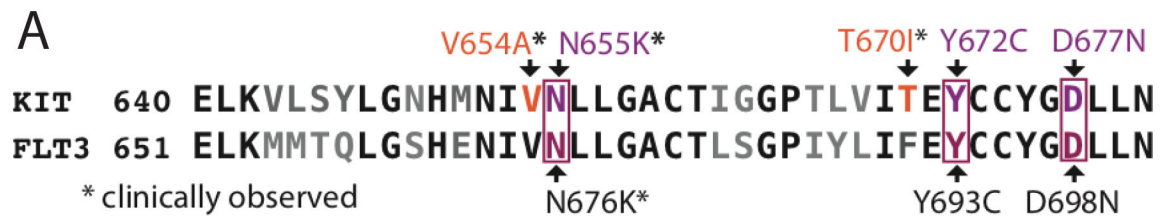
This study identifies potential problematic kinase domain mutations for next generation KIT inhibitors midostaurin and avapritinib.

Author Manuscript

Author Manuscript

Author Manuscript

Author Manuscript



primary activating mutation	KIT D816V*
resistance mutations previously found in KIT	KIT V654A* KIT T670I*
resistance mutations modeled from FLT3	KIT N655K* KIT Y672C KIT D677N

* clinically observed

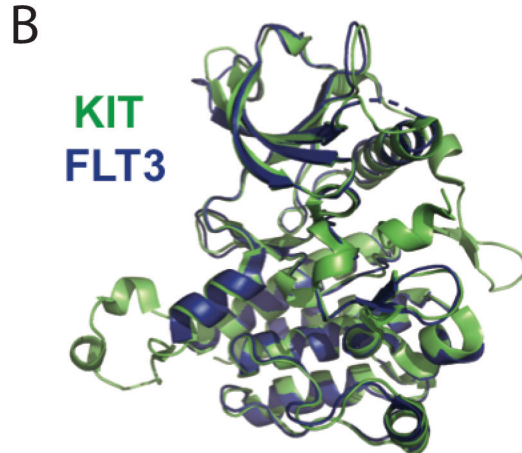


Figure 1. Candidate resistance mutations for midostaurin and avapritinib.

(A) Sequence alignment of KIT and FLT3 highlighting residues mutated in the KIT allelic series; mutations with prior evidence of resistance to KIT TKIs (orange) and mutations analogous to those in FLT3 that confer resistance to type I FLT3 TKIs (purple) are shown.

(B) Structural alignments of KIT (PDB: 4hvs) and FLT3 (PDB: 4XUF).

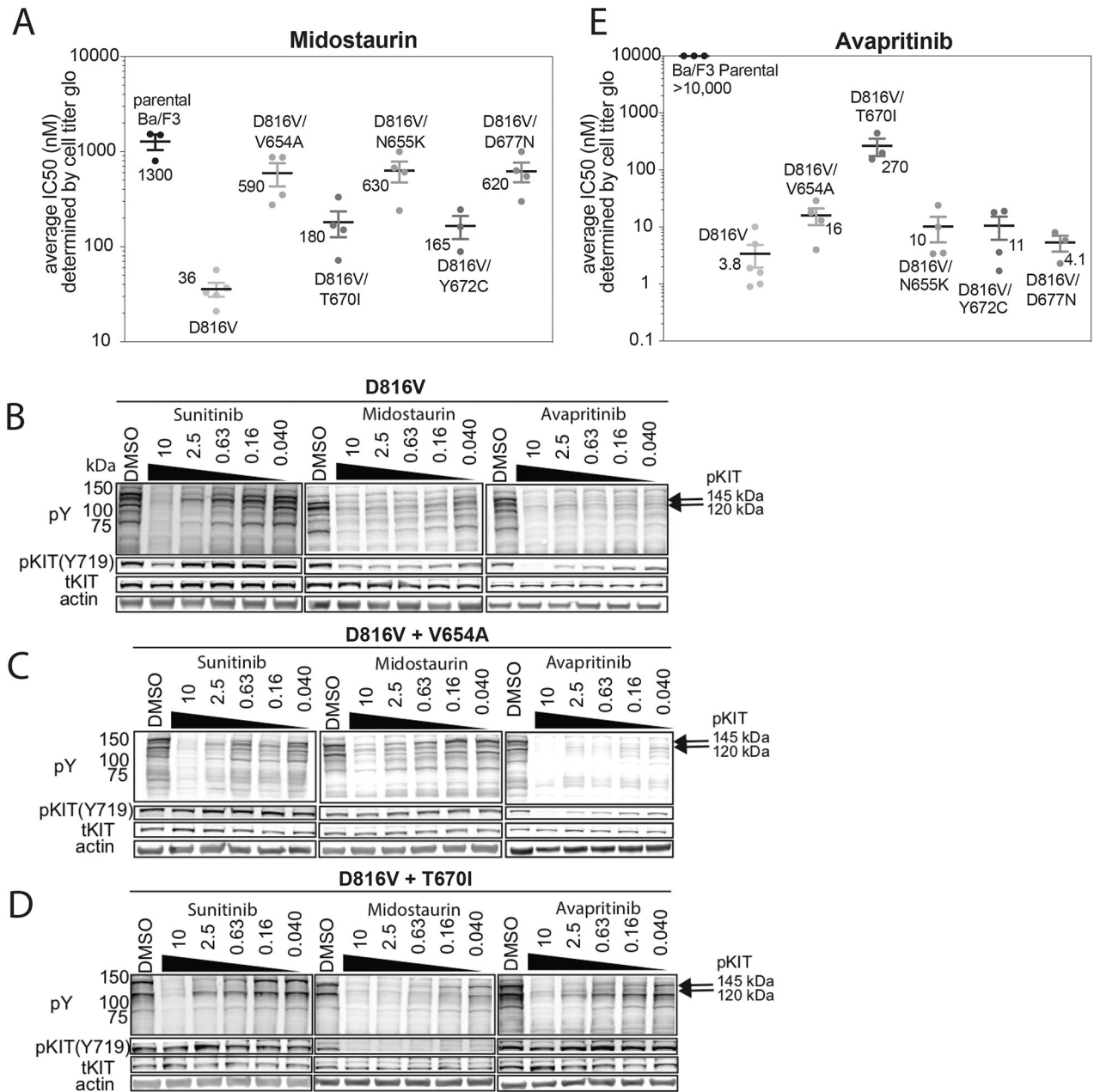


Figure 2. Midostaurin and avapritinib display non-overlapping resistance profiles.

Average IC50s of (A) midostaurin and (E) avapritinib in Ba/F3 cells expressing the D816V allelic series. Each data point represents one experiment done in triplicate. The average IC50 of at least 3 separate experiments is shown in nanomolar (nM). Western blot analysis of total phospho-tyrosine (pY) and pKIT in (B) Ba/F3 KIT D816V, (C) Ba/F3 KIT D816V/V654A and (D) Ba/F3 KIT D816V/T670I cells treated with sunitinib, midostaurin and avapritinib (0.040 to 10 μ M). Molecular weights are indicated adjacent to pY blots.

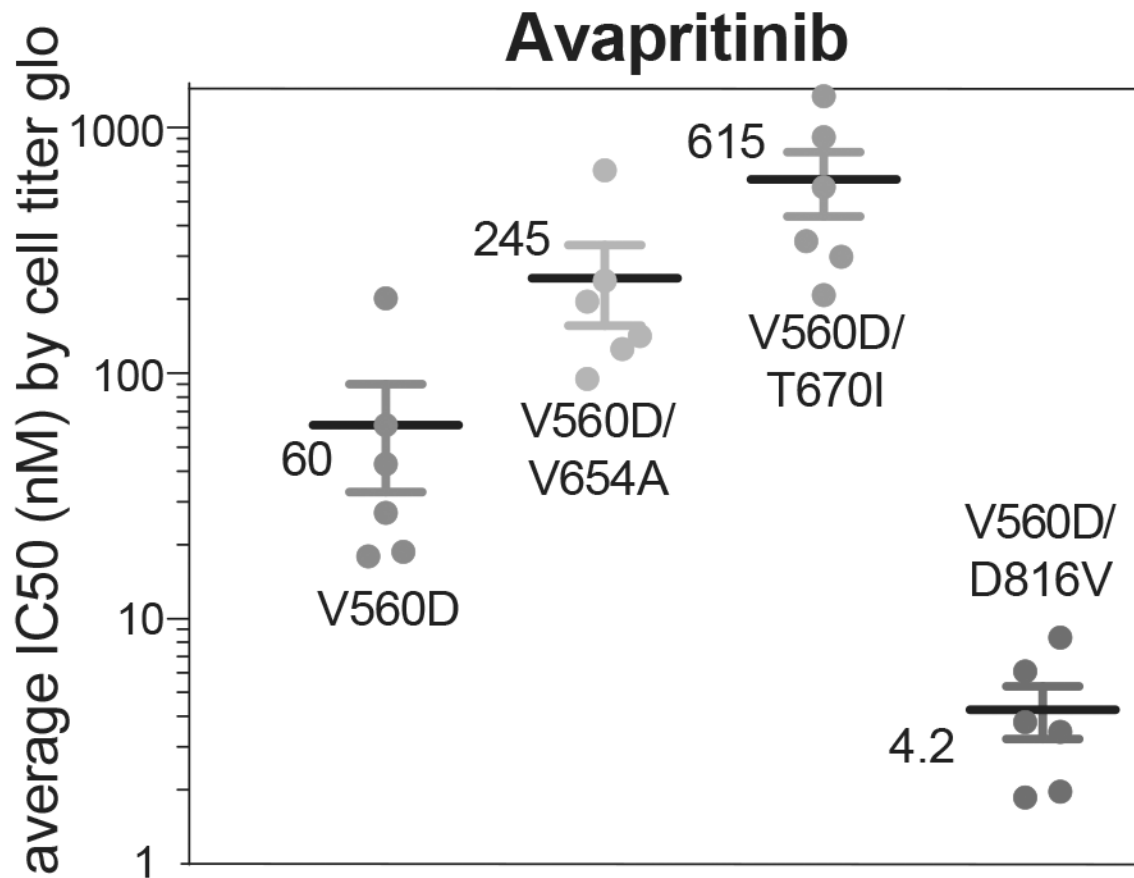


Figure 3. Avapritinib is less potent against KIT mutants with primary JM domain mutations. Average IC50s of avapritinib in Ba/F3 cells expressing the KIT V560D allelic series. Each data point represents one experiment done in triplicate. The average IC50 of at least 3 separate experiments is shown in nanomolar (nM).

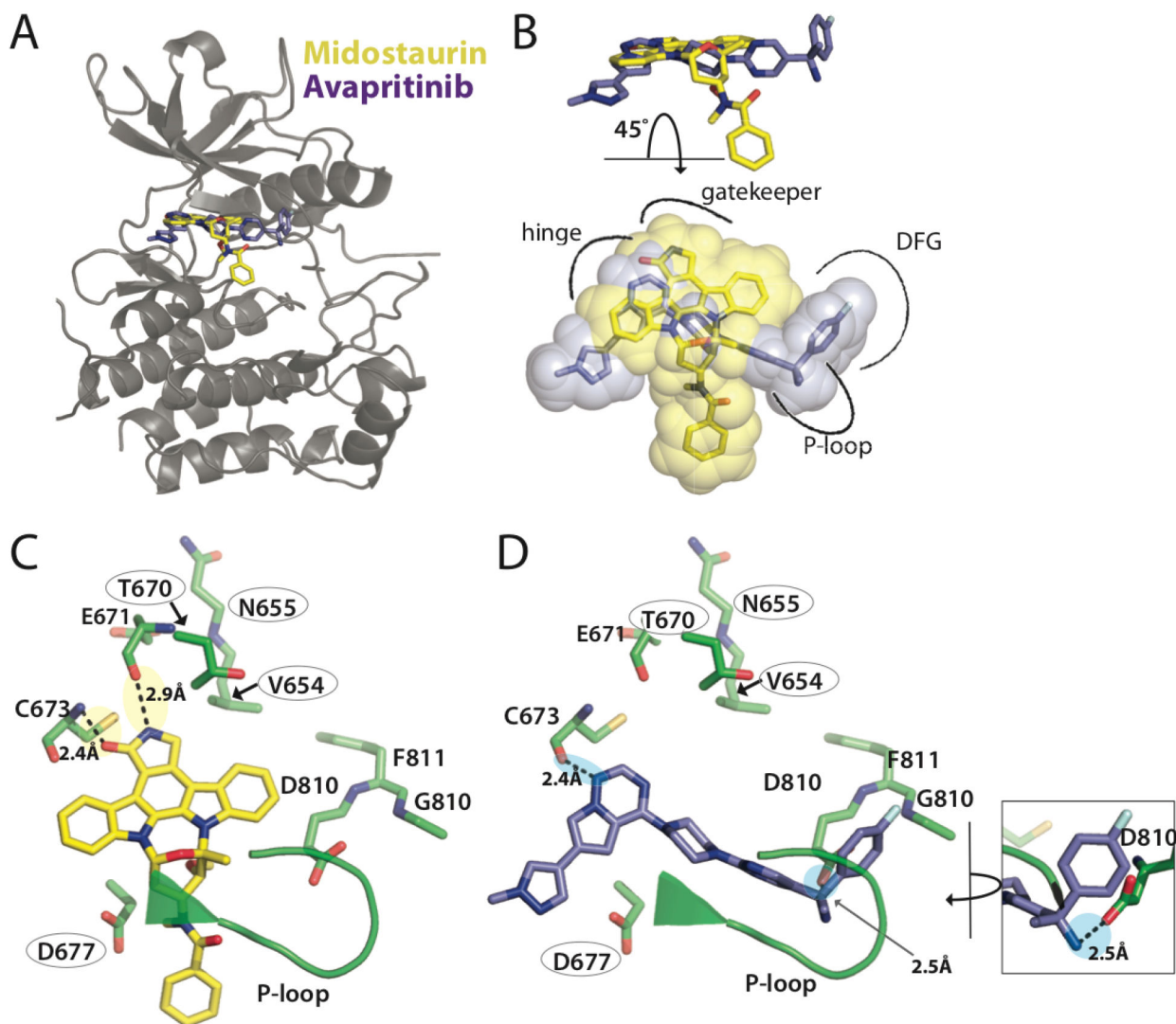


Figure 4. Molecular docking studies predict midostaurin and avapritinib have non-overlapping interactions with several residues in the active site of KIT D816V.

(A) Model of KIT D816V (grey) with docked poses of midostaurin (yellow) and avapritinib (blue). (B) Comparison of docked binding poses of midostaurin and avapritinib. Pockets within the KIT D816V active site represented by black curves labeled with corresponding structural features. Model of the binding positions of (C) midostaurin and (D) avapritinib in relation to residues V654, N655, T670 and D677 (circled) as well as the DFG motif and the P-loop. Predicted hydrogen bond between avapritinib and D810 of the DFG motif (D, zoomed panel). For the sake of clarity, only atoms discussed in the text, or backbone atoms between adjacent residues, are shown in (C) and (D). See Fig. S6 for more details on predicted binding pocket.

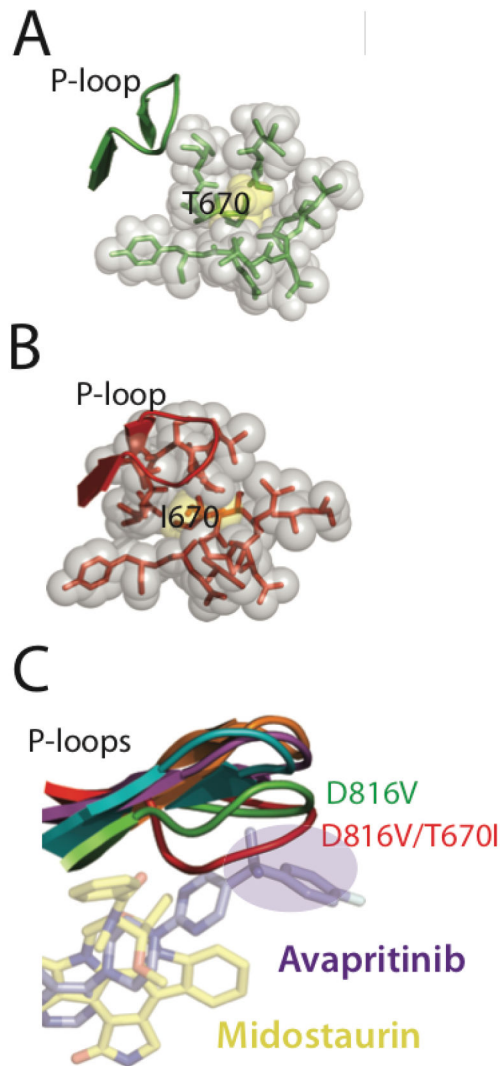


Figure 5. The presence of the T670I gatekeeper mutation is predicted to induce a distant conformational change in the P-loop.

Analysis of all residues within 4Å of residue 670 (yellow) in (A) D816V/T670 and (B) D816V/T670I. (C) Models comparing the P-loop conformation of KIT D816V/T670I (red) to the P-loop of KIT D816V (green) and the double mutants, D816V/V654A (orange), D816V/N655K (teal), and D816V/D677N (magenta). The pocket where the fluorophenyl moiety of avapritinib binds in the docked model is shown as a purple circle.

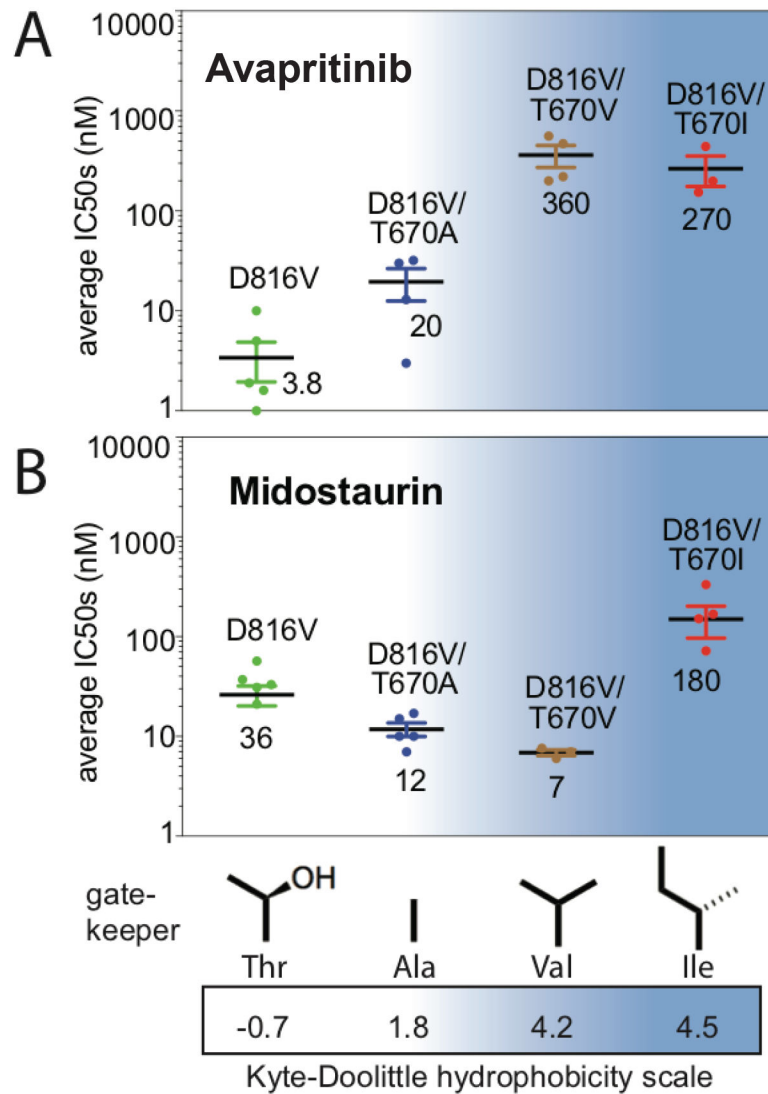


Figure 6. Increasing hydrophobicity of the gatekeeper residue correlates with increased resistance to avapritinib, but has minimal effect on midostaurin.

Average IC₅₀s of (A) avapritinib and (B) midostaurin against various gatekeeper mutants. Each data point represents one experiment done in triplicate. The average IC₅₀ of at least 3 separate experiments is shown in nM. The mutants are listed in order of increasing hydrophobicity of the gatekeeper residue, according to the Kyte-Doolittle hydrophobicity scale (58), as indicated by the blue gradient.